



Tailor-made material design: An evolutionary approach using multi-objective genetic algorithms

N. Chakraborti^{a,*}, R. Sreevathsan^a, R. Jayakanth^a, B. Bhattacharya^b

^aDepartment of Metallurgical and Materials Engineering, Indian Institute of Technology, Kharagpur, West Bengal 721 302, India

^bDepartment of Civil Engineering, Indian Institute of Technology, Kharagpur, West Bengal 721 302, India

ARTICLE INFO

Article history:

Received 21 September 2007
Received in revised form 4 March 2008
Accepted 4 March 2008
Available online 21 August 2008

Keywords:

Optimization
Materials design
Inter-atomic potential
Stiffness
Lightness
Lennard–Jones potential
Multi-objective genetic algorithms
NSGA-II

ABSTRACT

Materials design may be defined as designing materials as dynamic multilevel-structured systems with integrated and specific process/structure/performance/property relationships. The main objective of the work is to design structural materials based on inter-atomic potentials – the so-called “inverse problem” – to explore materials of high strength to weight ratio with a thermodynamically stable structure. Since the aforementioned objectives are contradicting each other it leads to a Pareto-optimal problem which is eventually solved by the multi-objective genetic algorithms solver NSGA-II. The material behavior is modeled using Lennard–Jones type interatomic potential function. The Pareto-optimal front provides a series of hypothetical materials which are then compared and contrasted with existing materials as and when possible.

© 2008 Elsevier B.V. All rights reserved.

1. Introduction

A study of mechanical properties of materials in terms of given interatomic potentials is of considerable interest since it provides a direct connection between the atomic structure and macroscopic behavior of the solid. This comes under the class of “forward problems”. A more interesting problem – and more challenging, is to come up with the ideal interatomic potentials that will give rise to a set of desirable material properties. This is the so-called “inverse problem” and is a relatively new approach to material design. The solution of the inverse problem has important implications in the control of self-assembly of many particle systems: through optimization one can create new materials that perhaps have not yet been reached in nature [1].

The present work is aimed at establishing a framework to design materials with a number of desirable qualities that are conflicting in nature. The idea is to come up with a procedure general enough to be extended to any set of mutually conflicting properties in a crystalline system. Mathematically this leads to a multi-objective problem [2], where in recent times the employment of evolutionary and genetic algorithms [3,4] have provided an excellent insight to a large number of problems in the mate-

rials domain [5–10]. The details of the optimization problem and the genetic procedure adopted in this work are detailed below.

2. The optimization problem

The aim of this study is to design some structural materials that are stiff, light and at the same time thermodynamically stable. The idea is to come up with the best possible tradeoffs between these conflicting requirements. The optimum solution in such a situation, as it is rather well established now [2], need not be unique. Rather a family of optimized solutions, formally known as the Pareto frontier [2] becomes the optimum here. Each member of this Pareto-set is an individually optimized solution of the same rank [3] as the others, and out of these available alternates the *decision makers* [2] should be able to pick one or more, based upon their own requirements.

In this study we have considered a three dimensional array of atoms following a prescribed crystallographic structure. All the three objectives here are modeled using the Lennard–Jones (L–J) potential function [11] – we acknowledge that this isotropic pair potential is selected mainly for its simplicity and the resulting mathematical tractability, and that the L–J potential may not be adequate for modeling most crystalline materials. Considering the requirements of the problem the three objectives are taken as:

* Corresponding author.

E-mail addresses: nchakrab@iitkgp.ac.in, nchakrab@metal.iitkgp.ernet.in (N. Chakraborti).

- Maximize Young's modulus, i.e., stiffness.
- Maximize the volume of the system with a requirement that the mass remains constant, i.e., maximize lightness or minimize density.
- Minimize the potential energy of the system so as to make it thermodynamically stable¹.

Two natural constraints are also prescribed: the Young's modulus must be non-negative and the L–J potential must be negative.

It should be intuitively clear that these objectives are mutually conflicting. For example, equilibrium energy and density: starting from the most stable configuration of a lattice, a lower density can be achieved only by increasing the inter-atomic distance and thereby increasing the energy of the system. Likewise, stiffness, which is the second derivative of the internal energy with respect to strain, can increase as the lattice is strained if the shape of the potential well is sharper than that of a square parabola. The cost is a higher energy as we go up the potential well.

Since Lennard–Jones potential governs all the three objectives, it is briefly discussed below for the convenience of the readers at large.

2.1. The Lennard–Jones potential

Neutral atoms and molecules experience two distinct forces in the limit of long and short distances – an attractive van der Waals force at long ranges, and a repulsion force, the result of overlapping electron orbitals, referred to as Pauli repulsion at short distances. The Lennard–Jones potential (also referred to as the 6–12 potential or, less commonly, 12–6 potential) is a simple mathematical model that represents this behavior:

$$E_{LJ} = 4\epsilon_0 \left[\left(\frac{\sigma}{r} \right)^a - \left(\frac{\sigma}{r} \right)^b \right], \quad (1)$$

where ϵ_0 is the depth of the potential well and σ is the (finite) distance at which the potential is zero. The commonly accepted values of the exponents a, b are 12, 6 respectively.

3. Modeling details

This study has been carried out for two common crystal symmetries, namely the body centered cubic (BCC) system with eight nearest neighbors and face centered cubic (FCC) system with 12 nearest neighbors. The number of unit cells considered for each lattice system is 8 and the number of atoms depends on the lattice structure considered. The temperature at which the properties are calculated is 0 K.

The systems were first modeled with all three parameters, a, b and σ as decision variables. To keep the computational cost within limits, only nearest neighbor interaction was considered between the atoms (instead of an atom interacting with all its neighbors within the cutoff radius of 2.5σ). However, this approach led to some unacceptably low volumes and high stiffnesses. An alternate strategy was therefore tried out.

In the alternate approach both a, b in the L–J potential function are kept constant at their standard values of 12 and 6 and σ remains the only decision variable. First, only nearest neighbors are

considered interacting with an atom; subsequently, all atoms within the cutoff radius (2.5 Å) are included. The following relationship between ϵ_0 and r_0 (the equilibrium distance), derived from real material properties [12,13], is used:

$$\epsilon_0 = \frac{\alpha + \beta f(r_0)}{\gamma + \delta e^{-\lambda \phi}}. \quad (2)$$

Values of the parameters $\alpha, \beta, \gamma, \delta$ and ϕ [12] are provided in Table 1. X denotes the number of atoms under consideration.

The cutoff radius depends on the assumed lattice symmetry (FCC, BCC) as the number and distance of nearest neighbors varies with lattice symmetry. Young's modulus, the first objective, was derived from some basic considerations detailed in Appendix I.

For nearest neighbor interaction model the Young's modulus is expressed as

$$Y = \frac{1}{V_0} \frac{\partial^2 E_{LJ}}{\partial \epsilon_{ij}^2} = \frac{1}{V_0} r_0^2 \left(\frac{\partial^2 E_{LJ}}{\partial \epsilon_{ij}^2} \right)_{r=r_0} = \frac{1}{r_0} \left(\frac{156\sigma^{12}}{r_0^{14}} - \frac{42\sigma^6}{r_0^8} \right) = \frac{156\sigma^{12}}{r_0^{15}} - \frac{42\sigma^6}{r_0^9}. \quad (3)$$

For a multiple atom interaction model it varies with the lattice structure based upon the number of nearest neighbors in each lattice structure. The expressions for BCC and FCC lattices are as follows:

For BCC lattice,

$$Y = \frac{1}{V_0} \left(\frac{\partial^2 E_{\text{Total}}}{\partial \epsilon_{ij}^2} \right)_{r=r_0} = \frac{4\epsilon_0}{a_L} \left[\frac{156\sigma^{12}}{r_0^{14}} - \frac{42\sigma^6}{r_0^8} \right] = \frac{4\sqrt{3}\epsilon_0}{2r_0} \left[\frac{156\sigma^{12}}{r_0^{14}} - \frac{42\sigma^6}{r_0^8} \right]. \quad (4)$$

For FCC lattice,

$$Y = \frac{1}{V_0} \left(\frac{\partial^2 E_{\text{Total}}}{\partial \epsilon_{ij}^2} \right)_{r=r_0} = \frac{4\epsilon_0}{a_L} \left[\frac{156\sigma^{12}}{r_0^{14}} - \frac{42\sigma^6}{r_0^8} \right] = \frac{4\epsilon_0}{\sqrt{2}r_0} \left[\frac{156\sigma^{12}}{r_0^{14}} - \frac{42\sigma^6}{r_0^8} \right]. \quad (5)$$

For atomic volume, the second objective, that we have attempted to maximize for a constant mass was simply calculated as

$$V = \begin{cases} a_L^3 & \text{for multiple atom interaction model} \\ r_0^3 & \text{for single atom pair interaction model} \end{cases}, \quad (6)$$

where the mass of the atom is assumed to be constant and a_L is the lattice parameter which has a structure dependent relationship with the equilibrium interatomic spacing r_0 .

For FCC, $a_L = \sqrt{2}r_0$ and for BCC it is $a_L = 2/\sqrt{3}r_0$.

Potential energy, the third objective was directly evaluated from Eq. (1).

3.1. Optimization strategy

In this study the tri-objective optimization has been carried out using the Non-dominated Sorting Genetic Algorithm II (NSGA II) [3] which applies the so called ' $(\mu + \lambda)$ – ES type of strategy' [3]

Table 1
Values of constants in Eq. (2)

Crystal lattice	BCC	FCC
α (eV)	1.37139×10^{-21}	3.75391×10^{-21}
β (eV)	1.54495×10^{-31}	1.17524×10^{-31}
γ	1.09467	0.43991
δ	–8.378421	–0.4745
ϕ	1.05169	0.372879

¹ Commonly in the materials literature thermodynamic stability is assessed through the value of Gibbs free energy (G). It remains a simple thermodynamic exercise to demonstrate that in the absence of any mechanical work, G becomes synonymous with Helmholtz's free energy (A). The value of A on the other hand is only slightly influenced by the entropy (S) contribution, in case of solids. Furthermore, as T equals 0 K, the situation considered here for the ease of computation, A becomes identical to the internal energy (U), which has been approximated by the L–J potential in this study.

in a multi-objective environment keeping the parent population size μ equal to the child population size λ . To elaborate further: a parent population of size μ is mixed with an offspring population of the same size, and only half of them are kept for the next generation following some specialized evolutionary strategies (ES) consisting of a *crowding distance tournament selection*, and in its later versions, a procedure for *controlled elitism*, both of which are aimed at preserving the population diversity, which are now adequately detailed in the literature [3].

A real coded simulated binary crossover – SBX [3] is used here with a probability of crossover 0.9. The mutation probability is taken as 0.5, the population size is fixed at 500 and the numbers of generations run are 10,000. All the computations are performed in a Windows XP environment.

4. Results and discussion

The major findings of this study are presented and analyzed below. The generated results are plotted and compared with real material properties which can give an initial idea for design of new materials.

Due to the problems with three variable approach mentioned earlier, further studies have been carried out with constant values of $a = 12$ and $b = 6$ for the L–J potential: σ is the only decision variable.

Figs. 1–4 show the Pareto frontiers and the corresponding energy contour plots for BCC and FCC structures. As indicated before, (i) both nearest neighbor interactions and (ii) all possible atomic interactions within the cutoff distance, have been considered. These results are compared with available information on a number of real materials [13], which are marked on the figures. All the real materials quite expectedly fall on the lower energy levels of these plots owing to their stable structures. The Pareto frontiers, however, seem to extend beyond these to lower energy levels, suggesting the possibility of designing new materials with even better thermodynamic stability and density–stiffness combinations. A material designer can, in addition to these three objectives, impose other constraints like cost to come up with a material of choice.

The findings are analyzed below in separate subsections.

4.1. Objectives based on nearest neighbor interactions

Both BCC and FCC symmetries were studied in this case. The results show a good agreement with the real material properties

[13]. The data for Vanadium, Molybdenum and Tungsten are superimposed over the computed results plotted in Fig. 3a and b. Among these three elements Tungsten appears to be superior in terms of its stiffness and lightness but being situated in the higher energy band, it is however inferior in terms of the thermodynamic stability compared to the other two. To design a material with better stiffness and lightness than Tungsten, one would require moving higher up in the energy level, so thermodynamic stability might be a potential problem. On the other hand Molybdenum is strategically located in a region surrounded by further lower energy levels and its lightness is of the same order as that of tungsten. The nature of the Pareto frontier in Fig. 3b shows the possibility of designing a material with the lightness comparable to Molybdenum but of stiffness and energy values better than it. This demonstrates a typical efficacy of the current evolutionary procedure in coming up with newer and better materials.

Fig. 2a shows the Pareto frontier for FCC lattice and the data for Gold, Copper, Platinum and Nickel are superimposed on the energy contour plot shown in Fig. 2b. It seems that all the four materials are at nearly comparable low energy states, Gold having the least stiffness. Since the low energy contours spread well beyond Gold, it seems quite possible to come up with a material with less stiffness and more lightness than Gold at a very comparable energetic stability. Once again this demonstrates how the current procedure could help in designing some newer materials with tailor-made properties. Though the L–J potential is relatively inaccurate for modeling metallic systems, these preliminary simulations show good agreement with real material properties as shown in Figs. 1–4.

4.2. Objectives involving all possible atomic interactions in a lattice

The results in Fig. 3a show the Pareto frontier for the BCC lattice structure and those in Fig. 3b show the real material properties superimposed on the contour plot of energy. These results are generated with the interaction of an atom with all its neighbors within a prescribed cut-off radius of 2.5σ beyond which the forces tend to become insignificant. Although more sophisticated interactions are considered here, the results essentially show the same trends as in the previous case, suggesting that the nearest neighbor interactions essentially drive the materials properties in the present context and configurations.

The Pareto frontier for the FCC lattice is shown in Fig. 4a and the elements plotted in the energy contour plot shown in Fig. 4b dem-

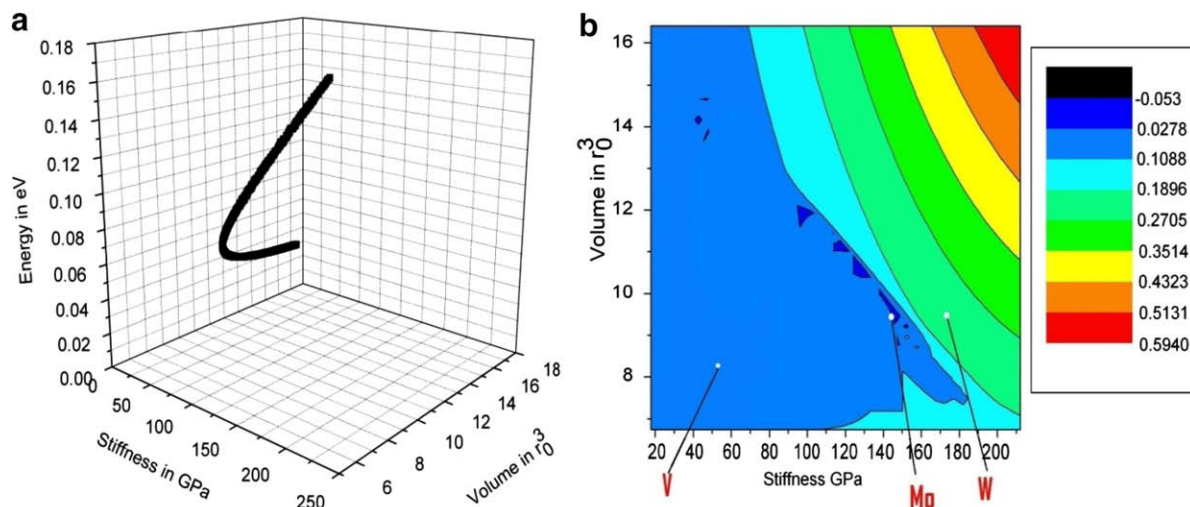


Fig. 1. (a) Pareto frontier for BCC structure with variable σ and nearest neighbor interaction model and (b) energy contour plot (in eV) for BCC with variable σ and nearest neighbor interaction model. The energy levels are color coded.

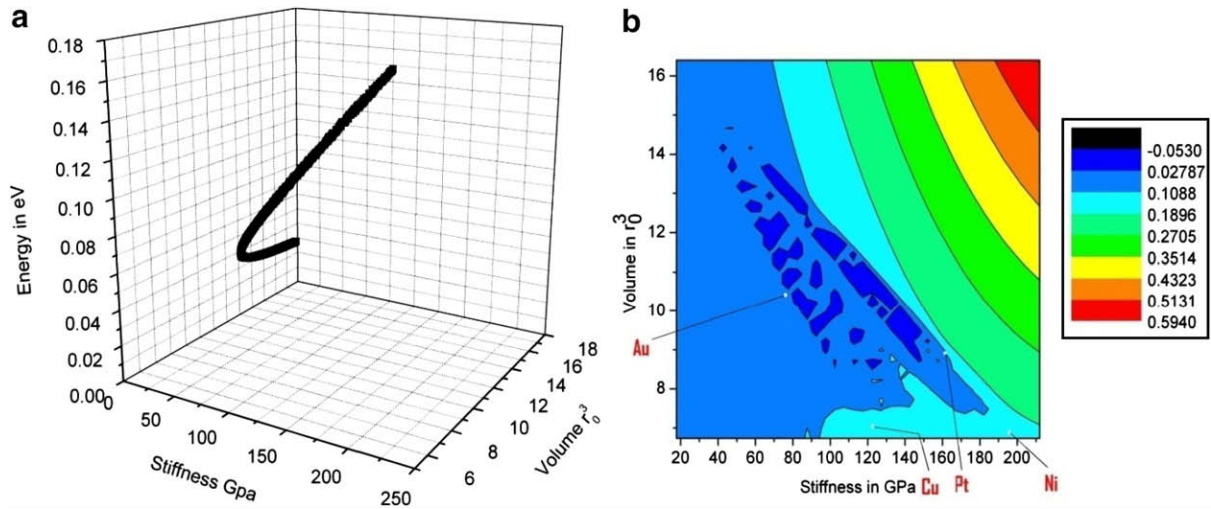


Fig. 2. (a) Pareto frontier for FCC structure with variable σ and nearest neighbor interaction model and (b) energy plot (in eV) for FCC with variable σ and nearest neighbor interaction model. The energy levels are color coded.

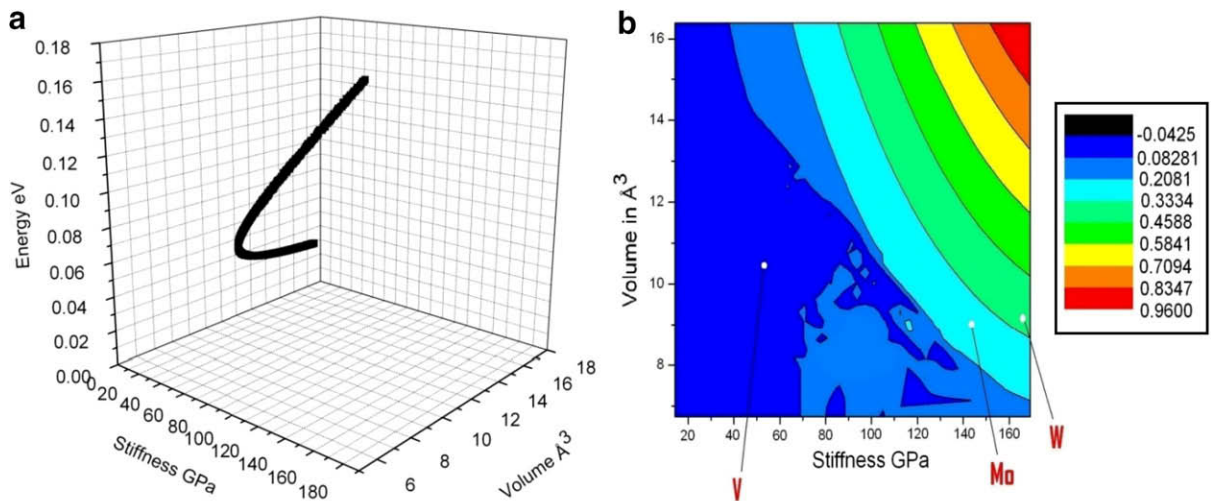


Fig. 3. (a) Pareto frontier for BCC structure with variable σ and cutoff radius interaction model and (b) energy plot (in eV) for BCC with variable σ and cutoff radius interaction model. The energy levels are color coded.

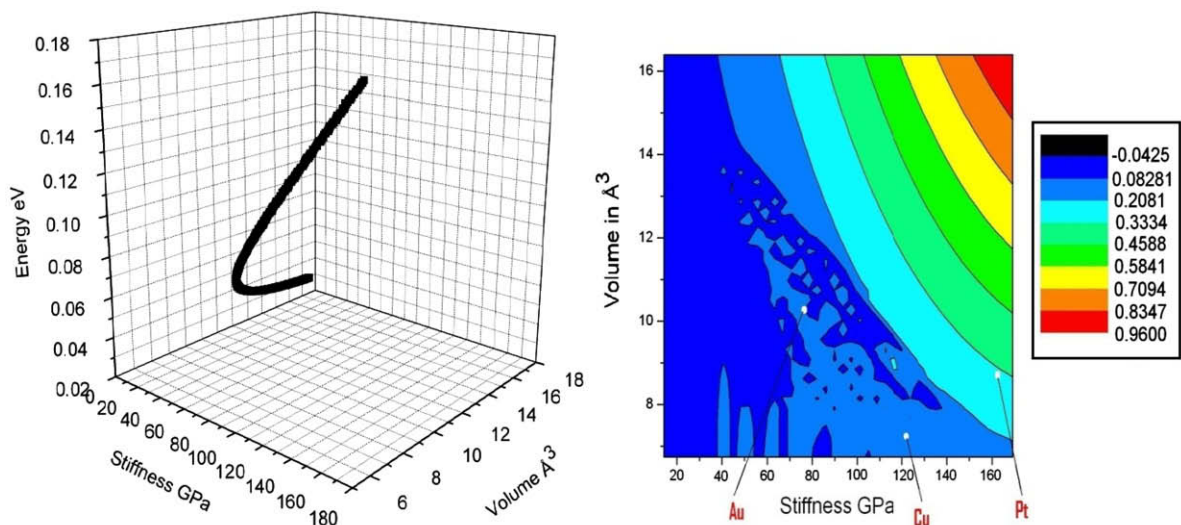


Fig. 4. (a) Pareto frontier for FCC structure with variable σ and cutoff radius interaction model and (b) energy plot (in eV) for FCC with variable σ and cutoff radius interaction model. The energy levels are color coded.

onstrates that the lowest energy contour actually extends to a lower stiffness level than what has been originally found considering just the 2-body interaction shown in Fig. 4b, demonstrating the possibility of designing materials less stiffer than gold for example, but with perhaps better lightness and stability.

4.3. Property correlations between BCC and FCC lattices

Fig. 5 describes the individual relationship between any two objectives when the third objective has a fixed set of values. The conflicting nature of the objectives has been clearly brought out

in these figures. For example, it is clear that at a given lightness, optimal stiffness can be increased only at the expense of increasing optimal equilibrium energy (Fig. 5a and b). Likewise, at fixed equilibrium energy, optimal stiffness can be increased only at the expense of decreasing optimal lightness (Fig. 5c and d). Finally, optimal equilibrium energy can be reduced and optimal lightness can be increased simultaneously without bound, but only at the cost of decreasing stiffness asymptotically towards zero (Fig. 5e and f). The optimized energy contours however show some significant local fluctuations, particularly at the lower energy level, as evident from Figs. 3b and 4b. Therefore, truly monotonic reduction

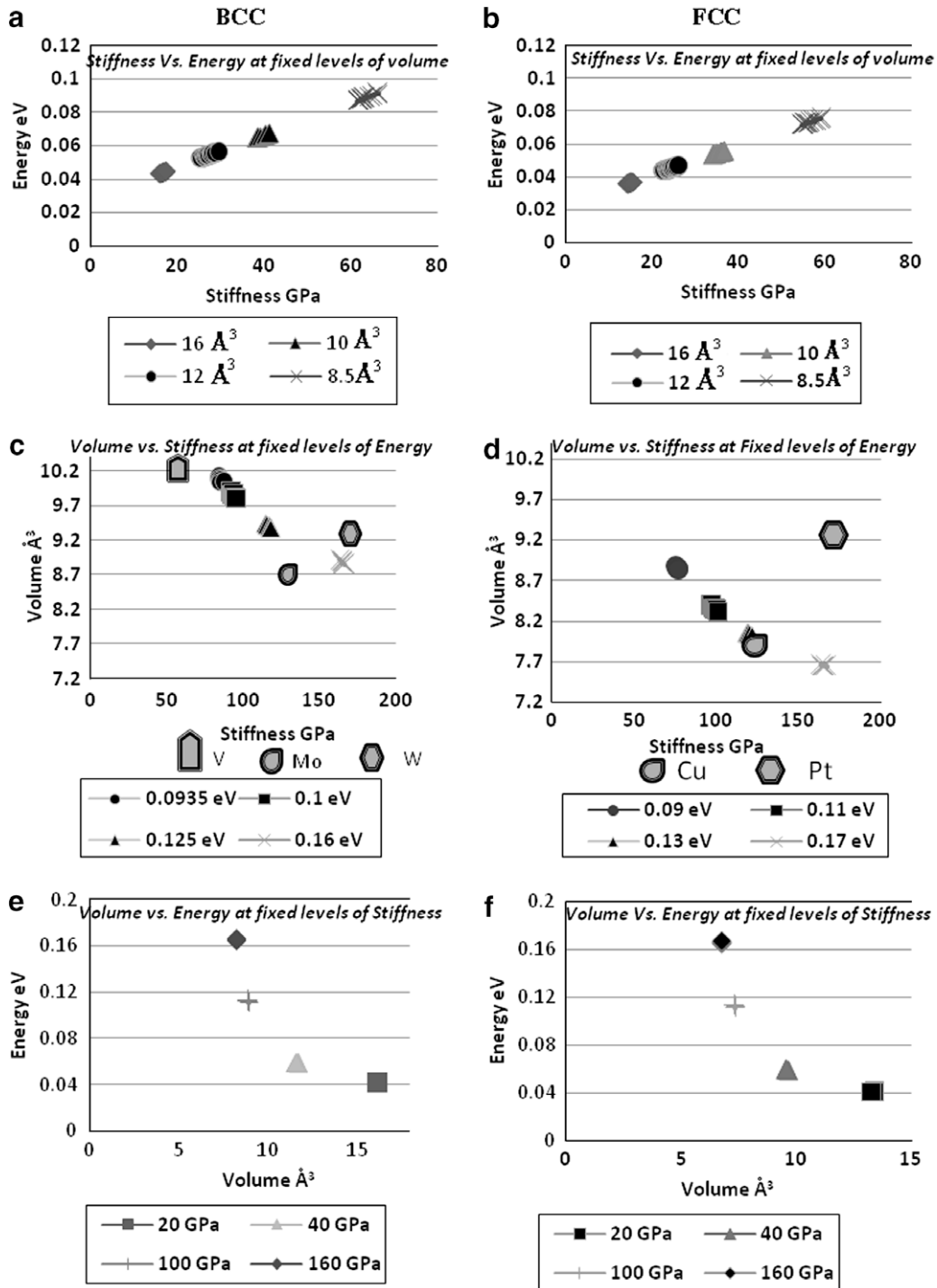


Fig. 5. Two objective correlations at fixed levels of another objective.

of energy might not be possible at all stiffness and lightness levels. Furthermore, a material could very well belong to a higher energy level compared to another and still be a legitimate member of the Pareto frontier, since a tradeoff needs to be worked out between all the three objectives. The relative positions of various elements shown in Fig. 5c and d corroborate these observations.

Fig. 5a and b shows the energy vs. stiffness relationship at similar volume scales, which clearly shows the higher stiffness of BCC materials over FCC materials. Molybdenum which belongs to the category of BCC materials has higher stiffness over Copper with FCC lattice structure at similar volume and energy levels plotted in Fig. 5c and d. Similarly the comparison between BCC-Tungsten and FCC-Platinum shows the same trend as described in the previous case. Fig. 5c and d clearly shows that BCC materials attain similar stiffness with FCC materials at a higher volume. The stiffness profiles in Fig. 5e and f show that at very similar energy levels, stiffness is higher for BCC materials at any volume considered.

5. Concluding remarks

The success of an inverse approach towards materials design with conflicting criteria is demonstrated here through the simple L–J potential. Since σ remains the only decision variable, the material design procedure for any target property combinations would just involve an adjustment of the lattice parameter of a particular cubic symmetry, rendering the material development task rather simple. The advantage of using a multi-objective genetic algorithm for this purpose is quite overwhelming. A logical extension of this work would be to try out some more sophisticated potentials and extend the procedure to materials of other categories, ionic melts and materials for example.

Appendix I. Derivation of an expression for the Young's modulus

The derivation of Young's modulus is carried out separately for different crystal lattices to include the structure dependence of the property.

The elastic tensor of a body is given by

$$C_{ijkl} = \frac{1}{V_0} \frac{\partial^2 E}{\partial \varepsilon_{ij} \partial \varepsilon_{kl}}, \quad (A1)$$

where V_0 is the reference volume, E is the total potential energy of the body and ε_{ij} is the strain tensor. The term Young's modulus, Y , stands for C_{1111} for an isotropic and linearly elastic material. For a nonlinear elastic material, we can take Y to be the initial slope of the axial stress vs. axial strain plot.

For a two-body interaction model the Young's modulus calculation is done as follows:

$$Y = \frac{1}{V_0} \left(\frac{\partial^2 E_{LJ}}{\partial \varepsilon_{ij}^2} \right), \quad (A2)$$

where Y is the Young's modulus of the material, E_{LJ} is L–J potential as given in Eq. (1) and ε_{ij} is the axial strain with respect to displacement from equilibrium interatomic distance r_0 .

From Eq. (A2)

$$\frac{\partial^2 E_{LJ}}{\partial \varepsilon_{ij}^2} = \frac{\partial^2 E_{LJ}}{\partial r^2} \left(\frac{\partial r}{\partial \varepsilon_{ij}} \right)^2. \quad (A3)$$

Assuming small displacements from the equilibrium position, the axial strain can be given as

$$\varepsilon_{ij} = \frac{r - r_0}{r_0}. \quad (A4)$$

Hence Eq. (A2) becomes

$$Y = \frac{1}{V_0} r_0^2 \left(\frac{\partial^2 E_{LJ}}{\partial r^2} \right)_{r=r_0}. \quad (A5)$$

The reference volume V_0 can be considered as the volume of a cube with sides r_0 in the free space between the two free atoms under consideration [14]. Thus the Young's modulus expression for a nearest neighbor interaction case can be expressed as

$$\begin{aligned} Y &= \frac{1}{r_0} \left(\frac{\partial^2 E_{LJ}}{\partial r^2} \right)_{r=r_0} = \frac{1}{r_0} \left(\frac{156\sigma^{12}}{r_0^{14}} - \frac{42\sigma^6}{r_0^8} \right) \\ &= \left(\frac{156\sigma^{12}}{r_0^{15}} - \frac{42\sigma^6}{r_0^9} \right). \end{aligned} \quad (A6)$$

When multiple atom interaction is considered as discussed in Section 3 separate expressions for BCC and FCC lattices have to be derived. The axial direction is taken to be [010]. The cut-off radius for the interatomic potential is considered to be 2.5σ in this work.

For an FCC lattice where each atom has 12 nearest neighbors the interaction potential is the summation of all interactions and hence can be given as

$$E_{\text{Total}} = \sum_{i=1}^{12} E_{LJ} = \sum_{i=1}^{12} 4\varepsilon_0 \left[\left(\frac{\sigma}{r_{i1}} \right)^{12} - \left(\frac{\sigma}{r_{i1}} \right)^6 \right], \quad (A7)$$

Where E_{Total} is the summation of potentials due to all the interactions within the cut-off radius.

Considering the four-way symmetry

$$\frac{\partial E_{\text{Total}}}{\partial \varepsilon_{ij}} = 4 \sum_{i=1}^{12} \left[\frac{\partial}{\partial \varepsilon_{i1}} \left(\frac{\sigma}{r_{i1}} \right)^{12} - \frac{\partial}{\partial \varepsilon_{i1}} \left(\frac{\sigma}{r_{i1}} \right)^6 \right]. \quad (A8)$$

The strain along the plane perpendicular to the stress plane becomes zero and the other two planes undergo different strains. Under these varying strains along different directions the following expression has been formulated for the Young's modulus of an FCC lattice as follows:

$$\begin{aligned} Y &= \frac{1}{V_0} \left(\frac{\partial^2 E_{\text{Total}}}{\partial \varepsilon_{ij}^2} \right)_{r=r_0} = \frac{4\varepsilon_0}{a_l} \left[\frac{156\sigma^{12}}{r_0^{14}} - \frac{42\sigma^6}{r_0^8} \right] \\ &= \frac{4\varepsilon_0}{\sqrt{2}r_0} \left[\frac{156\sigma^{12}}{r_0^{14}} - \frac{42\sigma^6}{r_0^8} \right]. \end{aligned} \quad (A9)$$

Similarly for a BCC lattice with eight nearest neighbors,

$$Y = \frac{1}{V_0} \left(\frac{\partial^2 E_{\text{Total}}}{\partial \varepsilon_{ij}^2} \right)_{r=r_0} = \frac{4\sqrt{3}\varepsilon_0}{2r_0} \left[\frac{156\sigma^{12}}{r_0^{14}} - \frac{42\sigma^6}{r_0^8} \right]. \quad (A10)$$

References

- [1] M.E. Kassner, N.S. Nasser, Z.G. Suo, G. Bao, J.C. Barbour, L.C. Brinson, H. Espinosa, H.J. Gao, S. Granick, P. Gumbsch, K.S. Kim, W. Knauss, L. Kubin, J. Langer, B.C. Larson, L. Mahadevan, A. Majumdar, S. Torquato, F.V. Swol, *Mech. Mater.* 37 (2005) 231–259.
- [2] K. Miettinen, *Non-Linear Multiobjective Optimization*, Kluwer Academic Publishers, Boston, 1999.
- [3] K. Deb, *Multi-Objective Optimization by Evolutionary Algorithms*, John Wiley & Sons, Chichester, 2001.
- [4] C.A. Coello, *Evolutionary Algorithms for Solving Multi-Objective Problems*, second ed., Springer Publications, New York, 2001.
- [5] K. Mitra, S. Majumdar, *Mater. Manuf. Process.* 22 (2007) 532–540.
- [6] B.V. Babu, J.H.S. Mubeen, P.G. Chakole, *Mater. Manuf. Process.* 22 (2007) 541–552.
- [7] K. Sastry, D.D. Johnson, A.L. Thompson, D.E. Goldberg, T.J. Martinez, J. Leiding, J. Owens, *Mater. Manuf. Process.* 22 (2007) 553–561.
- [8] H. Saxén, F. Petterson, K. Gunturu, *Mater. Manuf. Process.* 22 (2007) 577–584.
- [9] S.S. Sahay, R. Mehta, K. Krishnan, *Mater. Manuf. Process.* 22 (2007) 615–622.

- [10] S. Ganguly, S. Datta, N. Chakraborti, *Mater. Manuf. Process.* 22 (2007) 650–658.
- [11] C. Kittel, *Introduction to Solid State Physics*, John Wiley and Sons, Chichester, 1971.
- [12] M.M. Ali, *Pramana – J. Phy.* 53 (1999) 775–781.
- [13] A. Buch, *Pure-Metal Properties – A Scientific Technology Hand Book*, ASM International, Materials Park, Ohio, 1986. pp. 15–21.
- [14] N.W. Ashcroft, N.D. Mermin, *Solid State Physics*, Holt Rinehart and Winston Publishers, Orlando, Florida, 1977.